

Relation between three-dimensional echocardiography derived left ventricular volume and MRI derived circumferential strain in patients eligible for cardiac resynchronization therapy

Iris K. Rüssel · Jeroen van Dijk · Sebastiaan A. Kleijn ·
Tjeerd Germans · Gerjan de Roest · J. Tim Marcus ·
Otto Kamp · Marco J. W. Götte · Albert C. van Rossum

Received: 10 March 2008 / Accepted: 1 July 2008 / Published online: 17 July 2008
© The Author(s) 2008

Abstract *Objectives* To compare regional left ventricular (LV) volume curves obtained with real time three-dimensional echocardiography (RT3DE) with two-dimensional circumferential strain curves obtained by MRI in cardiac resynchronization therapy candidates. *Background* Several methods using either ultrasound or MRI are used to quantify mechanical dyssynchrony (MD). Theoretically, LV volume and circumferential strain seem related, since both measures are connected to the radius of the ventricle. *Methods* In 21 patients with chronic

heart failure, RT3DE and tagged MRI were performed subsequently. Regional LV volume was computed from the ultrasound images. From the MR images, regional circumferential strain was calculated. Cross-correlations with time lags of 1% of the cardiac cycle were performed to compare the curves in corresponding LV segments. Furthermore, peak septal to lateral (SL) delays were compared between modalities. *Results* High correlations were found between the curves ($r^2 = 0.65 \pm 0.19$), but regional differences in time delay between modalities were observed. In the septum, the volume curve was earlier than the strain curve by 1.8 ± 17.0 time-lags (n.s.), while in the lateral wall, the volume curve was earlier by 3.3 ± 12.0 time-lags ($P < 0.02$). There was a non-significant difference between SL delays in the two modalities (volume: $-1.0 \pm 8.6\%$, strain: $3.0 \pm 12.7\%$, $P = 0.17$, a positive sign indicates that the lateral wall is delayed). *Conclusions* High correlations were observed between both modalities, but regional differences in time-delay were found. This is possibly inherent to the method of echocardiographic volume calculation and hampers the comparison of both measures for the quantification of MD.

I. K. Rüssel (✉) · J. T. Marcus
Department of Physics and Medical Technology,
VU University Medical Center, De Boelelaan 1118,
1081 HV Amsterdam, The Netherlands
e-mail: i.russel@vumc.nl

I. K. Rüssel · T. Germans · G. de Roest · J. T. Marcus ·
M. J. W. Götte · A. C. van Rossum
Institute for Cardiovascular Research (IcaR-VU),
VU University Medical Center, Amsterdam,
The Netherlands

I. K. Rüssel · J. van Dijk · S. A. Kleijn · T. Germans ·
G. de Roest · O. Kamp · M. J. W. Götte ·
A. C. van Rossum
Department of Cardiology, VU University Medical
Center, Amsterdam, The Netherlands

J. van Dijk · S. A. Kleijn · O. Kamp · A. C. van Rossum
Interuniversity Cardiology Institute of the Netherlands
(ICIN), Utrecht, The Netherlands

Keywords Real-time 3D echocardiography ·
Myocardial tagging · Magnetic resonance imaging ·
Left ventricular volume · Left ventricular strain ·
Cardiac resynchronization therapy

Abbreviations

2D	Two-dimensional
3D	Three-dimensional
CRT	Cardiac resynchronization therapy
DCE	Delayed contrast enhancement
LV	Left ventricle
MRI	Magnetic resonance imaging

Introduction

Since only 70–80% of chronic heart failure patients receiving CRT respond to this therapy [1–5], better methods for prediction of response are mandatory. Mechanical dyssynchrony in LV contraction is thought to predict the response to CRT better than electrical dyssynchrony [6–8]. Both echocardiography and MRI are used to quantify mechanical dyssynchrony. While several measures of mechanical dyssynchrony are commonly used in ultrasound, such as tissue Doppler imaging (velocity [9, 10], strain [11]) or 3D-echo (volume [12, 13]), MRI predominantly focuses on circumferential strain [6, 14]. Myocardial strain is probably a more robust parameter for assessing mechanical dyssynchrony than regional wall motion or velocity, as it is less affected by overall heart motion and tethering [15].

In an animal study, circumferential strain was found to be a better measure of dyssynchrony than longitudinal strain [14]. MRI can probably best quantify circumferential strain since the heart can be imaged in any plane. However, this is a relatively time consuming approach.

Assessment of circumferential strain by ultrasound is limited due to the acoustic window and the angle of the ultrasound beam [15]. However, with the technique of real-time 3D-echocardiography, regional LV volume can be quantified during the whole cardiac cycle. This technique was found to provide fast and accurate quantification of mechanical dyssynchrony [12, 13].

Since both the strain assessment by MRI and the volume assessment by 3D-echocardiography have their own advantages for quantifying mechanical dyssynchrony and seem theoretically related, a comparison is useful.

The relation between LV volume and circumferential strain is thought to be as follows (see also the

Appendix): End-stage heart failure is often associated with a remodeled LV, which usually gets a more spherical shape. Because of this change in ventricular geometry, LV volume is probably dependent on the radius in these patients. LV circumferential strain is also directly related to the change in radius of the heart, since it describes the length changes in the circumference of the ventricle. Since both measures are dependent on the radius of the ventricle, it is expected that there will be a relation between (the third root of) the measured volume and the circumferential shortening of the LV. In this study, this relation is investigated. The result will give insight in whether it is likely that quantification of mechanical dyssynchrony performed with the less time-consuming 3D-echocardiography technique provides the same results as quantification of dyssynchrony with MRI circumferential strain. Furthermore, since myocardial scar changes tissue properties, the influence of the presence of scar tissue on the results is explored.

Methods

Subjects

A total of 21 patients referred for CRT were studied (age 64 ± 10 years, 10 male, 11 female). Patients were included according to the following selection criteria: ejection fraction (EF) $<35\%$, NYHA-class III–IV despite optimal pharmacological therapy, and sinus rhythm [16]. The patients had to be clinically stable and received standard heart failure therapy including diuretics, beta-blockers, angiotensin-converting enzyme inhibitors and/or ATII receptor blockers.

Furthermore, five healthy subjects (age 30 ± 5 years, 4 male, 1 female) with no history of cardiac disease were included as a control group.

Written informed consent was obtained according to our institutional guidelines (VU University Medical Center, Amsterdam, the Netherlands).

Transthoracic real-time 3D-echocardiography and regional volume

Ultrasound was performed using either a Sonos 7500 or iE33 echo machine (Philips Medical Systems, Eindhoven, the Netherlands) with a matrix transducer.

Transthoracic apical acquisitions were obtained during 5–7 s of breath hold, with a temporal resolution of 6–7 ms, while the patient was in left lateral position. The entire LV volume was included in the pyramid-shaped 3D scan-volume. For quantification of LV volumes, specially designed software was used (Research-Arena 1.2.2TM 4D-LV-Analysis, TomTec Imaging Systems, Munich, Germany).

In apical long-axis planes of the LV, endocardial contours were semi-automatically detected during the complete cardiac cycle. Based on these contours, a LV cast was created. The cast was divided into 16 pie-shaped segments, pointing towards a central line between the apex and center of the mitral valve, and 1 additional apical segment. The segments correspond to the 17-segment model as described by the American Heart Association [17]. For each segment, a volume curve was generated, starting at the R-top of the ECG. Only the first 16 segments were used for comparison.

MRI and regional circumferential strain

MR imaging was performed on a 1.5 T whole body system (Magnetom Sonata, Siemens, Erlangen, Germany). Complementary tagged (CSPAMM) myocardial images were acquired using steady state free precession imaging and a multiple brief expiration breath hold scheme as described before [18, 19]. Images for 2D strain analysis were acquired in three short-axis planes, evenly distributed over the LV, as planned on an end-systolic 4-chamber image. A retrospective triggered protocol was used with a temporal resolution of 15 ms.

For analysis of scar tissue, the delayed contrast enhancement (DCE) MRI technique was used in all patients. A contrast agent was administered after the tagging procedure (Gadolinium-DPTA, Magnevist, Schering AG, Berlin, Germany) with a dose of 0.2 mmol/kg. About 10 to 15 min after contrast

application, the LV was imaged in the same orientation as the tagged images using a segmented inversion-recovery gradient-echo pulse sequence. The inversion time was approximately 250 ms. Images were acquired in late diastole. The imaging parameters are given in Table 1.

From the tagged images, circumferential strain (ϵ_c) curves were obtained from the 50% mid-myocardial wall using the harmonic phase method [20] at 6 circumferential segments of each slice: inferoseptal, anteroseptal, anterior, anterolateral, inferolateral and inferior. The circumferential strain reflects the percent change in length of a small line segment in the circumferential direction over the cardiac cycle, with respect to end-diastolic length. The segments in the basal and mid-ventricular slice correspond to the first 12 segments of the 17-segment model used for echocardiography. The inferoseptal and anteroseptal segments in the apical slice were averaged to form one septal segment, the anterolateral and inferolateral segments were averaged to form one lateral segment, to become comparable to the segments 13–16 from the 17-segment echocardiography model (with the septal and lateral segments from MRI slightly larger than from echocardiography). Thus, a total of 16 segments were used for comparison.

Data analysis and statistics

The data of all 336 segments (16 segments \times 21 patients) were linearly inter- or extra-polated to obtain 100 data points per cardiac cycle, such that the time points in the cardiac cycle can be expressed as a percentage. Only the first 80% of the cardiac cycle was used for comparison, to eliminate the noise present in the last part of the strain curves, due to MRI tag fading.

RR-interval times were recorded during measurements with both modalities and compared using a paired Student's *t*-test.

Table 1 Imaging parameters

Acquisition	Voxel size (mm ³)	Matrix	Temporal resolution (ms)	α (°)	TR/TE (ms)	BW (Hz/pixel)
Tagging cines	1.2 \times 3.8 \times 6.0	256 \times 78	15	20	3.6/1.8	850
Conventional cines	1.3 \times 1.3 \times 6.0–8.0	256 \times 208	35–48	60	3.2/1.6	930
DCE images	1.6 \times 1.3 \times 5.0	208 \times 256	–	25	9.6/4.4	130

Matrix: number of readout \times phase encoding samples; α : excitation flip angle; TR: repetition time, TE: echo time; BW: receiver bandwidth

Subsequently, the cross-correlation r was calculated between the third root of the volume curves and the strain curves, using 35 time-lags, where 1 time-lag corresponds to 1% of the cardiac cycle length, in all the segments and slices. This means that the strain curve was shifted with respect to the volume curve for 35 time-lags in each direction. For the maximum cross-correlations in the segments, a regression analysis was performed for every segment over all patients. The squared maximum cross-correlation r^2 was used to calculate average values over patients. For regional information, average values were also calculated over the septal, anterior, lateral and inferior regions and over the slices. For efficiency reasons, results were not averaged over all segments separately.

Furthermore, times to peak volume and strain were determined from the volume and strain curves, again, as a percentage of the cardiac cycle. From this, the average septal and lateral times to peak were calculated and subtracted to give the septal to lateral delay for each subject. Septal to lateral delays were compared between both modalities using a paired t -test and Bland-Altman analysis was performed.

P -values lower than 0.05 were considered significant. Results are presented as mean \pm sd, unless indicated otherwise. Subsequently, the comparison was repeated while excluding segments that did not reach their overall maximum cross-correlation within the computed range of 35 time-lags. Finally, in the patients, it was explored whether there is a relation

between these curves and the presence or absence of fibrosis as assessed by DCE.

Results

In Table 2, characteristics and functional parameters of the heart failure patients and the healthy subjects are shown. Using the 3D echo 16-segment dyssynchrony index previously described by Kapetanakis et al. [13], 15 patients (71%) had significant mechanical dyssynchrony ($>3SD$ above the mean for normal subjects, which is 5.6% in our case).

The average RR-interval during 3D-ultrasound was 934 ± 96 ms versus 881 ± 99 ms during MRI. This was not statistically different ($P = 0.09$). Since each curve has 100 data points, on average, 1 time-lag corresponds to an intermodality delay of 9.1 ± 1.0 ms.

Cross-correlations

The average maximum cross-correlation between the volume obtained by 3D-ultrasound and the circumferential strain obtained by tagged MRI was $r^2 = 0.65 \pm 0.19$. The mean intermodality delay at maximum cross-correlation was -1.9 ± 12.4 time-lags, which is significant (95% confidence interval: -3.2 to -0.6 time-lags) and corresponds to an average time-delay of -16.9 ± 112.8 ms. The negative sign indicates that the strain curve was delayed

Table 2 Characteristics, medication and function parameters of the heart failure patients ($n = 21$) and the healthy subjects ($n = 5$)

Patient parameter	Value patients	Value healthy subjects
Age (yrs)	64 ± 10	30 ± 5
Sex (male/female)	10/11	4/1
Ischemic cardiomyopathy (n , %)	10, 48	
Diuretics (n , %)	15, 71	
Beta-blockers (n , %)	17, 81	
ACE-inhibitors (n , %)	19, 90	
ATII receptor blockers (n , %)	9, 43	
QRS width (ms)	132 ± 33	
QRS width ≥ 120 ms (n , %)	13, 62	
Heart rate (beat/min) during MRI	68 ± 7	69 ± 11
Heart rate (beat/min) during ultrasound	64 ± 6	69 ± 16
End-diastolic volume (ml)	172 ± 125	122 ± 35
End-systolic volume (ml)	62 ± 49	53 ± 14
Ejection fraction (%)	28 ± 6	56 ± 4
16-Segment dyssynchrony index (%) [13]	8.4 ± 3.7	3.5 ± 0.7

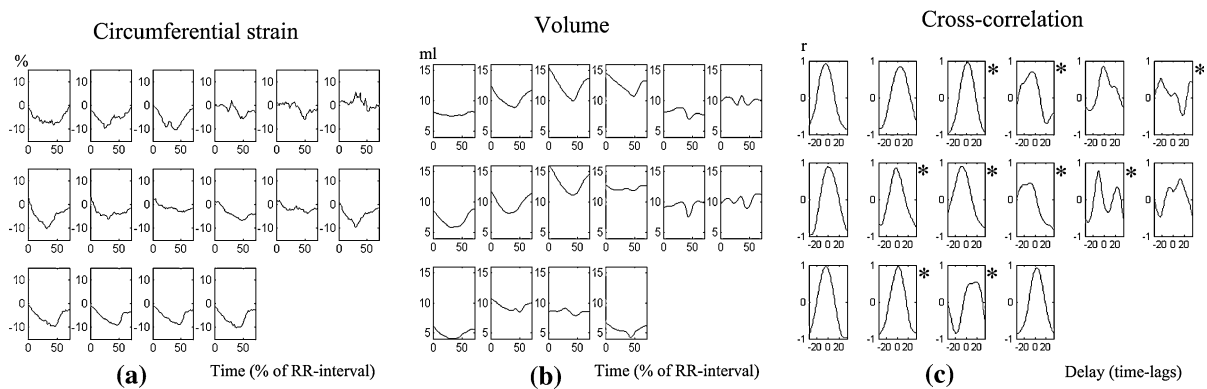


Fig. 1 Strain, volume and cross-correlation curves of all segments in one patient. From top to bottom: base, mid, apex. From left to right: inferoseptal, anterosseptal, anterior, anterolateral, inferolateral and inferior segments (apex: septal,

anterior, lateral, inferior). In the cross-correlation curves, a positive peak cross-correlation value depicts that the strain curve reached its peak before the volume curve. Cross-correlation curves marked with * indicate a segment with DCE

with respect to the volume curve. The accompanying average regression coefficient was $43.0 \pm 5.6\% \text{cm}^{-1}$ (mean \pm SE), and the constant was $-87.2 \pm 10.9\%$ (mean \pm SE). An example of the volume and strain curves and cross-correlations for one patient can be seen in Fig. 1.

In Table 3 and Fig. 2, the results for the separate regions are shown. Only in the lateral region of the mid-slice the cross-correlation delay was statistically different from 0 (95% confidence interval: -7.1 ± 3.1 time-lags (mean \pm SE)). Furthermore, regional differences in time-delays can be seen; some regions show negative delays, while others show positive delays. For example, the average intermodality delay in the septal region was -1.8 ± 17.0 time-lags (not significant), while the delay in the lateral region was -3.3 ± 12.0 time-lags ($P < 0.02$).

Septal to lateral delay

The average septal to lateral delay in the subjects was $-1.0 \pm 8.6\%$ of the cardiac cycle in the volume curves, and $3.0 \pm 12.7\%$ in the strain curves. The negative sign indicates that the septum was delayed with respect to the lateral wall in the volume curves, while the positive sign indicates that the lateral wall was delayed with respect to the septum in the strain curves. The difference between both modalities in septal to lateral delay was not significant: $P = 0.17$. A schematic illustration of regional differences and septal to lateral delays can be found in Fig. 3. Pearson correlation between septal to lateral delay in

both modalities was non-significant ($r = 0.34$, $P = 0.13$), and the mean difference between both measures was 4.0 ± 12.7 ms.

Table 3 Maximum cross-correlation results between 3D-echocardiography derived volume and 2D MRI derived circumferential strain per region for 336 segments

	Base	Mid	Apex
Septal			
r.c. ($\% \text{cm}^{-1}$)	42 ± 8	37 ± 4	33 ± 6
Con (%)	-85 ± 16	-72 ± 9	-65 ± 11
r^2	0.71 ± 0.19	0.71 ± 0.19	0.62 ± 0.20
Delay (lags)	-0.1 ± 16.4	-3.3 ± 16.3	-1.9 ± 17.9
Anterior			
r.c. ($\% \text{cm}^{-1}$)	37 ± 4	33 ± 4	34 ± 4
Con (%)	-78 ± 8	-69 ± 8	-69 ± 8
r^2	0.68 ± 0.18	0.69 ± 0.20	0.66 ± 0.26
Delay (lags)	1.8 ± 15.6	0.8 ± 15.1	-1.6 ± 15.3
Lateral			
r.c. ($\% \text{cm}^{-1}$)	67 ± 6	53 ± 5	41 ± 4
Con (%)	-138 ± 11	-109 ± 10	-86 ± 9
r^2	0.76 ± 0.22	0.73 ± 0.23	0.66 ± 0.25
Delay (lags)	-1.8 ± 11.1	-7.1 ± 10.1	-0.9 ± 13.9
Inferior			
r.c. ($\% \text{cm}^{-1}$)	53 ± 8	27 ± 3	34 ± 6
Con (%)	-99 ± 14	-55 ± 6	-66 ± 12
r^2	0.70 ± 0.21	0.66 ± 0.22	0.53 ± 0.26
Delay (lags)	-1.5 ± 12.7	-1.4 ± 13.5	-0.6 ± 20.1

Values are mean \pm SE for r.c.: regression coefficient; con: constant. Values are mean \pm sd for r^2 and the delay

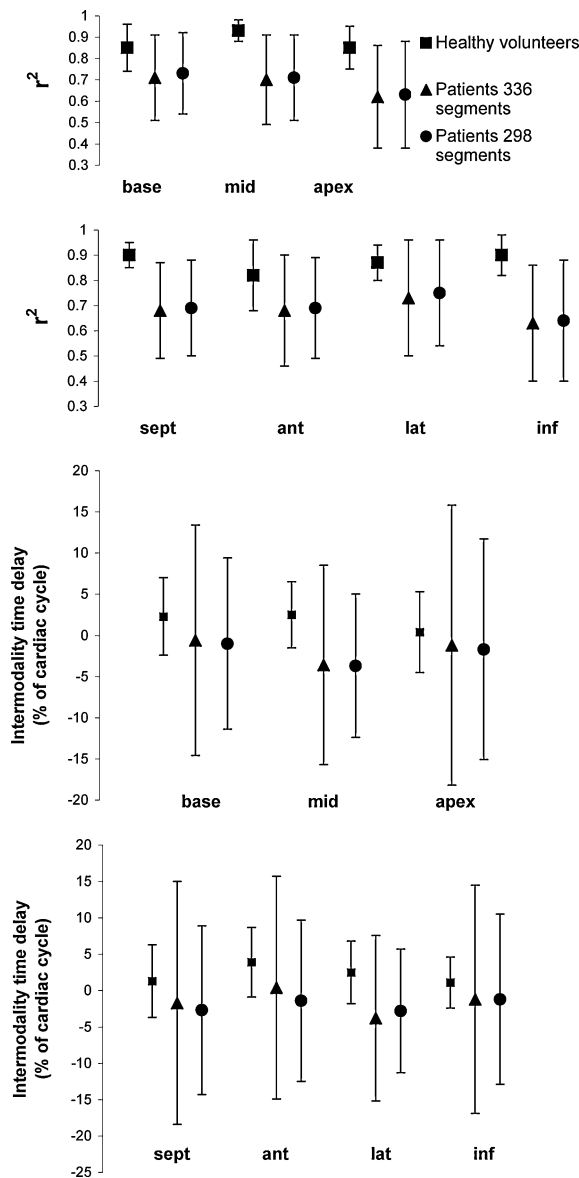


Fig. 2 Averaged regional r^2 and time-delay values. Averaged regional r^2 values for the maximum cross-correlations of the 5 healthy volunteers and 21 patients shown before and after exclusion of the 38 segments that did not reach a peak within the calculated time-lags. Also, the regional differences in time-delay between both modalities are shown. The error bars correspond to the SD. Sept: septal, ant: anterior, lat: lateral, inf: inferior

Segments with low cross-correlation

In 38 of the 336 segments (from 16 out of 21 patients), predominantly present in the septal region (Fig. 4), the cross-correlation curve did not reach its overall peak within the calculated time-lags. In 5 of

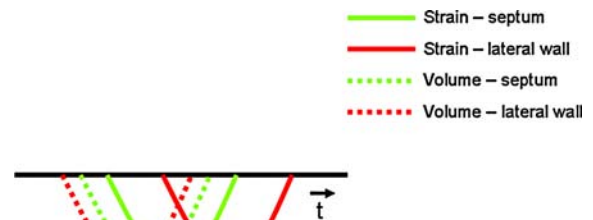


Fig. 3 Schematic illustration of regional differences between modalities and differences in septal to lateral delays. In both the septum and the lateral wall, the volume curve was delayed with respect to the strain curve. In the strain curves, the septum reached its peak before the lateral wall, whereas in the volume curves, the lateral wall reached its peak earlier

the segments, this was due to an unusual volume curve, whereas in 33 segments, this could be explained by the presence of a strain curve with very low or positive strain (“bulging”).

Cross-correlation after exclusion of ‘abnormal’ segments

The newly obtained average r^2 over 170 segments and time-delay values (Table 4) were not significantly different from the values obtained with 336 segments ($P = 0.28$). The standard deviation of the time delay, however, was significantly lowered ($P < 0.0001$). The mean maximum cross-correlation with 178 segments was $r^2 = 0.70 \pm 0.21$, with an average delay of -2.2 ± 10.7 time-lags, corresponding to -20.1 ± 96.6 ms. The accompanying average regression coefficient was $42.6 \pm 5.1\% \text{cm}^{-1}$ (mean \pm SE), and the constant was $-86.3 \pm 9.8\%$ (mean \pm SE). In Table 3 and Fig. 2, regional results are presented. Again, in the lateral region of the mid-slice the cross-correlation delay was significantly different from 0 (95% confidence interval: -4.9 ± 2.2 time-lags (mean \pm SE)). The regional differences in time-delays were reduced (septal: -2.5 ± 12.0 time-lags (n.s.), lateral: -2.4 ± 8.8 time-lags ($P < 0.03$)).

Septal to lateral delay after exclusion of ‘abnormal’ segments

After exclusion of the segments, the difference in septal to lateral delay between the modalities was also reduced. The septal to lateral delay in the volume

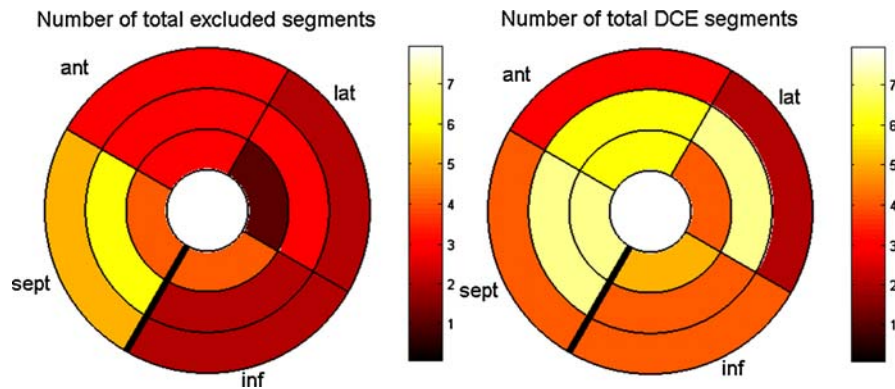


Fig. 4 Bulls-eye plots. Bulls-eye plots of the number of excluded segments (left) and number of segments with DCE (right). From the outside to the inside of the bulls-eye, the base, mid and apex slices are shown. Excluded segments are

predominantly located in the septal region. Segments showing DCE seem to be more evenly distributed, with a slight preference for the lateral region. Ant: anterior, lat: lateral, inf: inferior, sept: septum

Table 4 Maximum cross-correlation results between 3D-echocardiography derived volume and 2D MRI derived circumferential strain per region for 298 segments

	Base	Mid	Apex
Septal			
r.c. (%cm ⁻¹)	41 ± 8	37 ± 3	29 ± 4
Con (%)	-84 ± 16	-71 ± 6	-58 ± 8
r ²	0.72 ± 0.19	0.71 ± 0.19	0.64 ± 0.20
Delay (lags)	-0.9 ± 11.8	-5.2 ± 10.4	-1.5 ± 13.7
Anterior			
r.c. (%cm ⁻¹)	39 ± 4	33 ± 3	34 ± 5
Con (%)	-85 ± 8	-67 ± 5	-68 ± 8
r ²	0.70 ± 0.17	0.71 ± 0.16	0.65 ± 0.26
Delay (lags)	0.9 ± 11.0	-0.7 ± 8.4	-4.3 ± 13.3
Lateral			
r.c. (%cm ⁻¹)	67 ± 6	54 ± 5	43 ± 5
Con (%)	-137 ± 11	-112 ± 9	-91 ± 9
r ²	0.78 ± 0.18	0.77 ± 0.20	0.69 ± 0.25
Delay (lags)	-1.7 ± 8.9	-5.0 ± 6.9	-0.6 ± 10.3
Inferior			
r.c. (%cm ⁻¹)	47 ± 6	27 ± 3	32 ± 5
Con (%)	-92 ± 13	-53 ± 6	-60 ± 9
r ²	0.72 ± 0.20	0.66 ± 0.23	0.54 ± 0.27
Delay (lags)	-1.6 ± 9.4	-1.4 ± 8.8	-0.5 ± 15.6

Values are mean ± SE for r.c.: regression coefficient; con: constant. Values are mean ± sd for r² and the delay

curves was $-0.7 \pm 7.3\%$ of the cardiac cycle and $0.5 \pm 12.7\%$ in the strain curves ($P = 0.64$). Pearson correlation between septal to lateral delay in both modalities remained the same after exclusion of the

segments ($r = 0.35$, $P = 0.12$), but the mean difference between both measures decreased to 1.3 ± 12.2 ms.

Healthy subjects

In the healthy subjects, 80 segments (16 segments × 5 subjects) were compared. RR-intervals were not significantly different between the two measurements (Table 2, $P > 0.98$), and the 16-segment dyssynchrony index was similar to the value reported by Kapetanakis et al. [13] ($3.5 \pm 0.7\%$ vs. $3.5 \pm 1.8\%$, respectively).

The average maximum cross-correlation was $r^2 = 0.88 \pm 0.09$, and the mean intermodality delay was 1.9 ± 4.3 time-lags, corresponding to 16.5 ± 37.3 ms. The regression coefficient was $35.2 \pm 1.6\% \text{cm}^{-1}$ (mean ± SE), and the constant $-65.5 \pm 2.7\%$ (mean ± SE). Regional r^2 -values and intermodality time-delays can be found in Fig. 2.

The septal to lateral delay in the healthy subjects was $4.5 \pm 4.2\%$ of the cardiac cycle in the strain curves, and $1.2 \pm 3.0\%$ in the volume curves ($P = 0.20$). Pearson correlation between the septal to lateral delays was not significant ($r = 0.13$, $P = 0.83$), and the mean difference was 3.3 ± 4.9 ms.

DCE

In 10 of the patients, scar tissue was identified based on observed DCE in the MR images. In general, the location of the DCE seemed not to be related to the location of the excluded segments (Fig. 4). DCE was

observed in only 4 of the excluded segments (out of 3 patients), while a total of 59 segments showed DCE (out of 10 patients). Segments with DCE showed normal cross-correlation curves (Fig. 1).

Discussion

In this study, the curves of regional change in LV volume and circumferential strain as obtained with 3D-ultrasound and tagged MRI, respectively, were compared. In addition, the influence of scar tissue on the relation was explored. The results show that the correlation between the curves is relatively high, but that there are regional differences in time-delay between curves derived from both techniques. Furthermore, there is a difference between septal to lateral delays measured with both modalities (Fig. 3). The presence of abnormal, positive circumferential strain, indicating stretch or “bulging”, causes poor cross-correlation curves. Areas of delayed enhancement, indicating scar tissue, seem not related to these curves. Exclusion of these curves led to a significant reduction in the standard deviation of the time-delay, less regional difference in time-delay and more similarity in septal to lateral delay between the methods, but not to better correlation. In healthy volunteers with no signs of dyssynchrony, correlation was higher and less regional difference in time-delay was observed.

Heart rate

The difference in heart rate of the subjects between the subsequent measurement modalities might have influenced the results. The time points in the cardiac cycle were expressed as a percentage. Since it is known that shortening or lengthening of the RR interval mainly influences the length of the diastolic part of the cardiac cycle [21, 22], some shifts between the curves from the two modalities could have been expected. However, the differences in heart rate were not found to be statistically significant. Furthermore, this would only lead to a shift in one direction, not to the observed regional differences in time-delay. However, it is not fully known how the different parts of the cardiac cycle are altered at varying heart rates in patients with a dyssynchronous contraction.

Cross-correlations

Even though the measured maximum cross-correlations were high, it is no proof of equality. For the quantification of mechanical dyssynchrony, regional information on time delay, such as the septal to lateral delay, is by far more important. Intermodality delays differed between the tested regions, and had a negative sign on average (Fig. 2). This implicates that the values of mechanical dyssynchrony might be over- or under-estimated with respect to the other imaging modality. This was shown by the septal to lateral delay, which surprisingly had a different sign in both modalities, but was not found to be significantly different. Furthermore, the standard deviations of the maximum cross-correlations and accompanying time-delays were relatively large, indicating a substantial amount of variation between the comparisons.

In the healthy subjects, there was also some regional variation in time-delay (Fig. 2). However, in this case the delays had a positive sign and the standard deviations were very low compared to the patient group. The regional time-delay differences might have been caused by the non-fixed reference centerline used for the volume calculations. It is known from literature [23], that circumferential strain is somewhat larger in the anterior region. Our results show that the largest intermodality delay occurs in this region. If the regional volume curves become more balanced because of the moving reference centerline, this may result in regional variation in time-delay between both measurements.

The same effect might have played a role in the measured septal to lateral delays. In the healthy subjects, this delay was larger in the strain measurements.

Segments with low cross-correlation

The most striking finding was the poor cross-correlation between the volume curves and the segments with little or positive circumferential strain, indicating dyskinesia or “bulging”, which are commonly found in CRT candidates. Apparently, there is little resemblance between regional lengthening (“bulging”) and change in volume. This discrepancy seems to have great influence on the observed regional differences in time delay and on the septal to lateral delay as shown in Fig. 3.

Once again, a possible explanation for this finding could be the non-fixed center line in the 3D LV volume cast of the ultrasound measurements. Circumferential lengthening in patients with a dyssynchronous contraction can be caused by the counteracting opposite region. In other words, the region that shows lengthening, is pushed away by the opposite wall. When in this case the center line of the LV volume cast moves to the center of both walls, no regional increase in volume will be observed and the volume curve will appear more normal.

Therefore, it might be concluded that the postulation of a direct relationship between circumferential strain calculated from MRI tagging and regional volume calculated from 3D ultrasound is not valid in patients these patients, and that 3D echo and MRI strain represent different, not directly related measures of mechanical dyssynchrony.

Clinical implications

After the exclusion of the segments with low cross-correlation, no significant change in maximum cross-correlation was observed. The SD of the time delay on the other hand, decreased significantly, and the septal to lateral delay became more similar, indicating that exclusion of the poorly correlating segments had a positive effect on the overall comparison of MRI derived LV circumferential strain and 3D-ultrasound derived LV volume. Nevertheless, the need to exclude segments to make good comparisons is undesirable in clinical practice, and the difference seems to be caused by the regional volume calculation in 3D ultrasound. Moreover, these regional contraction patterns are characteristic for patients with a dyssynchronous contraction pattern. Considering the much better results obtained in the control group, MRI strain and 3D echo volume might represent different measures of mechanical dyssynchrony, which are intrinsic to the regional volume calculation. On the other hand, the finding that the presence of DCE did not influence the cross-correlation between the two measurement methods could be considered an advantage, because comparison seems correct in segments with scar tissue.

Limitations

A possible limitation is the inter- or intra-observer variability in the contouring of the myocardium. For

the ultrasound measurements, this variability was found to be low [24]. For the tagged MR images, a study using the harmonic phase method showed good inter- and intra-observer variability [25]. We only included the midwall layer in the strain analysis, since this region is expected to contain mainly circumferentially oriented myofibers [26]. In the reproducibility study [25], it was shown that inter- and intra-observer agreement were best in the mid-wall layer and increased with improved image quality. In our study, only subjects with good image quality on both modalities were included.

3D-echocardiography and MRI

In previous studies comparing ultrasound and MRI dyssynchrony measurements, good correlations were found [27, 28]. However, in contrast to this study, in these cases no different measures were compared. Both studies compared the similarity of velocity measurements in ultrasound and MRI. In the comparison of real-time 3D-echocardiography and MRI, global LV function and regional wall motion were found to correlate well between the two modalities [29, 30]. It requires further study, which modality or technique will be superior for predicting the response to CRT. Furthermore, strain analysis is focusing on the deformation in the cardiac wall, whereas in the volume measurements in 3D-ultrasound, only the endocardial border is used. Besides, regional change in LV volume seems influenced by the moving centerline in the volume measurement.

Conclusion

High cross-correlations were observed between regional MRI derived LV circumferential strain and real-time 3D-echocardiography derived regional LV volume. However, regional differences in time delay between the curves were found, leading to discrepancies in the quantification of mechanical dyssynchrony. This could mainly be ascribed to the poor correlation between regions with little or positive circumferential strain (dyskinesia or “bulging”) and the accompanying regional volume curves, and is probably inherent to the calculation method of regional LV volume. Therefore, both modalities

might represent different measures of mechanical dyssynchrony.

Acknowledgement Grant support: The Netherlands Organisation for Health Research and Development, grant number 945-05-016.

Open Access This article is distributed under the terms of the Creative Commons Attribution Noncommercial License which permits any noncommercial use, distribution, and reproduction in any medium, provided the original author(s) and source are credited.

Appendix

The relation between LV volume and circumferential strain is thought to be as follows:

The remodeled, more spherical heart will have a volume V as a sphere:

$$V = \frac{4}{3}\pi r^3 \quad (1)$$

Circumferential strain describes the length changes in the circumference of the LV ($2\pi r$). Assuming a circular ventricle with homogeneous strain, the circumferential length change ε_c can be represented as:

$$\varepsilon_c = \frac{r_n - r_1}{r_1}, \quad (2)$$

where r is the radius and n a time point in the cardiac cycle. In this equation, r_1 can be considered as a constant term.

Since both volume and circumferential strain are dependent on the radius of the heart, a relation between the third root of the volume and the circumferential strain is expected.

References

- Achilli A, Peraldo C, Sassara M, Orazi S, Bianchi S, Laurenzi F (2006) Response to cardiac resynchronization therapy: The selection of candidates for CRT (SCART) study. *Pacing Clin Electrophysiol* 29:S11–S19. doi: [10.1111/j.1540-8159.2006.00486.x](https://doi.org/10.1111/j.1540-8159.2006.00486.x)
- Bax JJ, Abraham T, Barold SS, Breithardt OA, Fung JW, Garrigue S (2005) Cardiac resynchronization therapy: Part 1—issues before device implantation. *J Am Coll Cardiol* 46:2153–2167. doi: [10.1016/j.jacc.2005.09.019](https://doi.org/10.1016/j.jacc.2005.09.019)
- Vernooy K, Verbeek X, Peschar M et al (2005) Left bundle branch block induces ventricular remodelling and functional septal hypoperfusion. *Eur Heart J* 26:92–98
- Yu CM, Abraham WT, Bax JJ, Chung E, Fedewa M, Ghio S (2005) Predictors of response to cardiac resynchronization therapy (PROSPECT)—study design. *Am Heart J* 149:600–605. doi: [10.1016/j.ahj.2004.12.013](https://doi.org/10.1016/j.ahj.2004.12.013)
- Swedberg K, Cleland J, Dargie H et al (2005) Guidelines for the diagnosis and treatment of chronic heart failure: executive summary (update 2005). *Eur Heart J* 26:1115–1140. doi: [10.1093/eurheartj/ehi166](https://doi.org/10.1093/eurheartj/ehi166)
- Nelson GS, Curry CW, Wyman BT et al (2000) Predictors of systolic augmentation from left ventricular preexcitation in patients with dilated cardiomyopathy and intraventricular conduction delay. *Circulation* 101:2703–2709
- Yu Y, Kramer A, Spinelli J, Ding J, Hoersch W, Auricchio A (2003) Biventricular mechanical asynchrony predicts hemodynamic effect of uni- and biventricular pacing. *Am J Physiol Heart Circ Physiol* 285:H2788–H2796
- Bax JJ, Bleeker GB, Marwick TH et al (2004) Left ventricular dyssynchrony predicts response and prognosis after cardiac resynchronization therapy. *J Am Coll Cardiol* 44:1834–1840. doi: [10.1016/j.jacc.2004.08.016](https://doi.org/10.1016/j.jacc.2004.08.016)
- Yu CM, Zhang Q, Fung JW, Chan HC, Chan YS, Yip GW (2005) A novel tool to assess systolic asynchrony and identify responders of cardiac resynchronization therapy by tissue synchronization imaging. *J Am Coll Cardiol* 45:677–684. doi: [10.1016/j.jacc.2004.12.003](https://doi.org/10.1016/j.jacc.2004.12.003)
- Yu CM, Fung JW, Zhang Q, Chan CK, Chan YS, Lin H (2004) Tissue Doppler imaging is superior to strain rate imaging and postsystolic shortening on the prediction of reverse remodeling in both ischemic and nonischemic heart failure after cardiac resynchronization therapy. *Circulation* 110:66–73. doi: [10.1161/01.CIR.0000133276.45198.A5](https://doi.org/10.1161/01.CIR.0000133276.45198.A5)
- Sogaard P, Egeblad H, Kim WY, Jensen HK, Pedersen AK, Kristensen BO (2002) Tissue Doppler imaging predicts improved systolic performance and reversed left ventricular remodeling during long-term cardiac resynchronization therapy. *J Am Coll Cardiol* 40:723–730. doi: [10.1016/S0735-1097\(02\)02010-7](https://doi.org/10.1016/S0735-1097(02)02010-7)
- van Dijk J, Mannaerts HFJ, Visser CA, Kamp O (2005) Evaluation of global and regional left ventricular function with real time 3D echocardiography in patients with an isolated left bundle branch block. *Circulation* 112(Supplement 2):403–404. doi: [10.1161/CIRCULATIONAHA.104.506337](https://doi.org/10.1161/CIRCULATIONAHA.104.506337)
- Kapetanakis S, Kearney MT, Siva A, Gall N, Cooklin M, Monaghan MJ (2005) Real-time three-dimensional echocardiography: a novel technique to quantify global left ventricular mechanical dyssynchrony. *Circulation* 112:992–1000. doi: [10.1161/CIRCULATIONAHA.104.474445](https://doi.org/10.1161/CIRCULATIONAHA.104.474445)
- Helm RH, Leclercq C, Faris OP (2005) Cardiac dyssynchrony analysis using circumferential versus longitudinal strain: implications for assessing cardiac resynchronization. *Circulation* 111:2760–2767. doi: [10.1161/CIRCULATIONAHA.104.508457](https://doi.org/10.1161/CIRCULATIONAHA.104.508457)
- Herbots L, Maes F, D'hooge J et al (2004) Quantifying myocardial deformation throughout the cardiac cycle: a comparison of ultrasound strain rate, grey-scale M-mode and magnetic resonance imaging. *Ultrasound Med Biol* 30:591–598. doi: [10.1016/j.ultrasmedbio.2004.02.003](https://doi.org/10.1016/j.ultrasmedbio.2004.02.003)
- Strickberger SA, Conti J, Daoud EG, Havranek E (2005) Patient selection for cardiac resynchronization therapy. *Circulation* 111:2760–2767. doi: [10.1161/01.CIR.0000161276.09685.4A](https://doi.org/10.1161/01.CIR.0000161276.09685.4A)

17. Cerqueira MD, Weismann NJ, Dilsizian V, Jacobs AK, Kaul S (2002) Standardized myocardial segmentation and nomenclature for tomographic imaging of the heart. *Circulation* 105:539–542. doi:[10.1161/hc0402.102975](https://doi.org/10.1161/hc0402.102975)
18. Zwanenburg JJM, Kuijter JPA, Marcus JT, Heethaar RM (2003) Steady state free precession with myocardial tagging: CSPAMM in a single breathhold. *Magn Reson Med* 49:722–730. doi:[10.1002/mrm.10422](https://doi.org/10.1002/mrm.10422)
19. Zwanenburg JJM, Gotte MJW, Kuijter JPA, Heethaar RM, van Rossum AC, Marcus JT (2004) Timing of cardiac contraction in humans mapped by high-temporal-resolution MRI tagging: early onset and late peak of shortening in the lateral wall. *Am J Physiol Heart Circ Physiol* 286:H1872–H1880. doi:[10.1152/ajpheart.01047.2003](https://doi.org/10.1152/ajpheart.01047.2003)
20. Osman NF, Prince JL (1998) Direct calculation of 2D components of myocardial strain using sinusoidal MR tagging. In: *Proceedings of SPIE Medical Imaging Conference*. San Diego, pp 142–152
21. Royse CF, Royse AG, Wong CT, Soeding PF (2003) The effect of pericardial restraint, atrial pacing, and increased heart rate on left ventricular systolic and diastolic function in patients undergoing cardiac surgery. *Anesth Analg* 96:1274–1279. doi:[10.1213/01.ANE.0000055801.23956.C2](https://doi.org/10.1213/01.ANE.0000055801.23956.C2)
22. Lavine SJ, Krishnaswami V, Levinson N, Shaver JA (1988) Effect of heart rate alterations produced by atrial pacing on the pattern of diastolic filling in normal subjects. *Am J Cardiol* 62:1098–1102. doi:[10.1016/0002-9149\(88\)90556-5](https://doi.org/10.1016/0002-9149(88)90556-5)
23. Young AA, Kramer CM, Ferrari VA, Axel L, Reickeck N (1994) Three-dimensional left ventricular deformation in hypertrophic cardiomyopathy. *Circulation* 90:854–867
24. van Dijk J, Dijkmans PA, Gotte MJW, Spreeuwenberg MD, Visser CA, Kamp O (2008) Evaluation of global left ventricular function and mechanical dyssynchrony in patients with an asymptomatic left bundle branch block: a real-time 3D echocardiography study. *Eur J Echocardiogr* 9:40–46
25. Castillo E, Osman NF, Rosen BD et al (2005) Quantitative assessment of regional myocardial function with MR-tagging in a multi-center study: interobserver and intraobserver agreement of fast strain analysis with Harmonic Phase (HARP) MRI. *J Cardiovasc Magn Reson* 7:783–791. doi:[10.1080/10976640500295417](https://doi.org/10.1080/10976640500295417)
26. Wyman BT, Hunter WC, Prinzen FW, McVeigh ER (1999) Mapping propagation of mechanical activation in the paced heart with MRI tagging. *Am J Physiol Heart Circ Physiol* 276:H881–H891
27. Delfino JG, Bhasin M, Cole R et al (2006) Comparison of myocardial velocities obtained with magnetic resonance phase velocity mapping and tissue Doppler imaging in normal subjects and patients with left ventricular dyssynchrony. *J Magn Res Im* 24:304–311. doi:[10.1002/jmri.20641](https://doi.org/10.1002/jmri.20641)
28. Westenberg JJ, Lamb HJ, van der Geest RJ et al (2006) Assessment of left ventricular dyssynchrony in patients with conduction delay and idiopathic dilated cardiomyopathy: head-to-head comparison between tissue Doppler imaging and velocity encoded magnetic resonance imaging. *J Am Coll Cardiol* 47:2042–2048. doi:[10.1016/j.jacc.2006.01.058](https://doi.org/10.1016/j.jacc.2006.01.058)
29. Joachim Nesser H, Sugeng L, Corsi C et al (2007) Volumetric analysis of regional left ventricular function with real-time three-dimensional echocardiography: validation by magnetic resonance and clinical utility testing. *Heart* 93:572–578. doi:[10.1136/hrt.2006.096040](https://doi.org/10.1136/hrt.2006.096040)
30. Corsi C, Coon P, Goonewardena S et al (2006) Quantification of left ventricular wall motion from real-time 3-dimensional echocardiography in patients with poor acoustic windows: effects of contrast enhancement tested against cardiac magnetic resonance. *J Am Soc Echocardiogr* 19:886–893. doi:[10.1016/j.echo.2006.02.010](https://doi.org/10.1016/j.echo.2006.02.010)